JOURNAL OF APPLIED ELECTROCHEMISTRY 15 (1985) 431–439

Concentration of carbon dioxide by a high-temperature electrochemical membrane cell

M. P. KANG*, J. WINNICK

School of Chemical Engineering, Georgia Institute of Technology, Atlanta, Georgia 30332, USA

Received 7 June 1984; revised 15 August 1984

The electrochemical carbon dioxide concentrator has emerged over the last few years as the best technique for carbon dioxide control in a manned spacecraft. Preliminary investigations have shown that the Molten Carbonate Fuel Cell (MCFC) can be successfully converted into a molten carbonate CO_2 concentrator (MCCDC) for CO_2 removal from a space-cabin [1]. The present investigation involved studying the MCCDC cell performance without use of a fuel for anode depolarization. Cathode CO_2 removal efficiencies of 97% were achieved with 0.25% CO_2 inlet concentration. Anode CO_2 concentrations were as high as 3.4% for 0.25% CO_2 and 5.8% for 1% CO_2 inlet concentration. Anode polarizations were approximately four times higher than cathode polarizations, which are considerably higher than in the MCFC. Anode exchange current densities were much smaller than cathode exchange current densities, suggesting poor anode–electrolyte contact. The total mathematical model consists of simple cathode and anode representations, combining activation and gas-phase diffusion. This treatment is capable of accurately correlating cell performance as a function of the process variables, such as flow-rate, temperature, and CO_2 inlet concentration.

1. Introduction

Expendable adsorption processes (LiOH cartridges) have been used in the Mercury, Gemini, Apollo and Space Shuttle manned missions. As the length of manned space missions increases, the cost of these expendables will become prohibitive due to increased weight and volume penalties. The development of regenerative processes for the revitalization of spacecraft atmospheres are therefore required.

The early Space Shuttle program marked the optional use of regenerative techniques for CO_2 collection with a solid amine for the three enhanced-orbiter missions. The Skylab program marked the beginning of the use of regenerative techniques for CO_2 collection from a spacecraft cabin atmosphere using cyclic adsorption/desorption beds containing commercial zeolites [2]. The emerging requirement for maintaining the CO_2 content of a spacecraft atmosphere at a CO_2 partial pressure ($p\,CO_2$) below 400 Pa (3 mmHg) made the zeolite systems unattractive, due to their resulting high weight and volume penalties [3].

The aqueous alkaline fuel cell has been successfully converted into use as an aqueous CO_2 concentrator for air-quality control in manned spacecraft [4]. The aqueous concentrator utilizing caesium carbonate (Cs_2CO_3) as the electrolyte performed successfully with relative humidities above 60%. Electrodes were of noble metals. At lower relative humidities, drying of the electrolyte occurs and the electrolyte precipitates at the anode. The success of the aqueous CO_2 concentrator suggests the use of a similar device utilizing a molten salt electrolyte which offers the advantages of insensitivity to relative humidity, non-noble electrodes, and high current efficiency at high current densities.

The molten carbonate fuel cell is a natural CO_2 transfer device, e.g. [5, 6]. The standard oxidant gas composition 70% air/30% CO_2 (dry) with the CO_2/O_2 ratio of 2, is fed to the fuel-cell. As a result the molten-carbonate fuel cells consume

Present address: NASA-Lewis Research Center, Cleveland, OH 44122, USA.

0021–891X/85 $03.00 + .12

CO_2 at the cathode and discharge it at the anode. Thus, the cathode-inlet gas stream must contain enough CO_2 to support the electrochemical process, while the anode effluent is CO_2-rich. For a cost-effective molten-carbonate fuel-cell system, the CO_2 contained in the anode effluent needs to be transferred to the cathode inlet.

Hydrogen is used as fuel at the anode

$$H_2 + CO_3^{2-} = H_2O + CO_2 + 2e \qquad (1)$$

The reaction occurring at the cathode is

$$CO_2 + 1/2\,O_2 + 2e = CO_3^{2-} \qquad (2)$$

Owing to the loss of carbonate at the anode, this gas is passed along with air to the porous cathode where the carbonate ion is formed. The overall reaction governing the open-circuit for the cell is

$$H_2 + 1/2\,O_2 = H_2O \qquad (3)$$

This device was successfully tested as a CO_2 concentrator [7, 8]. The oxidant is the simulated cabin atmosphere, in this case containing no recycle CO_2 from the anode. This low-level CO_2 was removed at high efficiency from the simulated cabin atmosphere at levels below 400 Pa. The anode product, a concentrated mixture of H_2, CO_2, CO and water vapour would be utilized in a Bosch, Sabatier or similar reactor to provide make-up water. The carbonaceous product, carbon or methane, would be stored or dumped. There are, however, mission profiles where use of hydrogen as a fuel is uneconomic. In these cases, electric power would be available to drive the concentration process. While the cathodic process remains the same an entirely new anodic situation exists in the absence of hydrogen as a depolarizer. Operation of a molten carbonate cell in this manner, even with high CO_2 oxidant levels, has not been previously reported.

2. Theory

2.1. *Molten carbonate CO_2 concentrator (MCCDC) – driven cell*

In the application of the MCFC to the task of the MCCDC, the oxidant must approximate the actual cabin atmosphere. In the driven-cell mode, an air mixture with low CO_2 concentration is supplied into the cathode. Nitrogen as inert gas is used to purge the product at the anode.

In this cell, an external power supply is added to the system in order to drive the cell reaction. The system functions as a true concentration cell. The overall reaction becomes simply

$$(CO_2)_c + (1/2\,O_2)_c + 2e = (CO_2)_a + (1/2\,O_2)_a + 2e \qquad (4)$$

The dependence of the equilibrium potential on the activities of oxygen and carbon dioxide can be described by the Nernst equation:

$$E_e = \frac{RT}{2F} \ln \left\{ \left[\frac{(a_{CO_2})\,(a_{O_2})^{1/2}}{(a_{CO_3^{2-}})} \right]_a \times \left[\frac{(a_{CO_3^{2-}})}{(a_{O_2})^{1/2}\,(a_{CO_2})} \right]_c \right\} \qquad (5)$$

Assuming the activities of carbonate anion to be unity,

$$E_e = \frac{RT}{2F} \ln \left\{ \frac{[(a_{O_2})^{1/2}(a_{CO_2})]_a}{[(a_{O_2})^{1/2}(a_{CO_2})]_c} \right\} \qquad (6)$$

2.2. *Electrokinetics*

Development of a fuel cell as a CO_2 concentrator requires knowledge of the behaviour under very low cathode CO_2 partial pressures. Reaction (2) has been studied both in free electrolyte [9] and in a membrane [10]. The cathodic reaction orders in CO_2 are approximately -1 in free carbonate electrolyte on gold electrodes and close to zero in the membrane cell with porous NiO electrodes. In both cases the reaction order for oxygen is about 0.5. The low reaction order in CO_2 is ideally suited to the operation of the MCFC as a CO_2 concentrator because CO_2 is removed from a gas mixture (CO_2/O_2) with very low CO_2 partial pressure (e.g., 0.005 atm). Thus the kinetics for CO_2 reduction remain high even at very low inlet CO_2 partial pressure. These results suggest that the MCCDC should have power densities of the same order as the MCFC with a low inlet CO_2 partial pressure.

The anode reaction mechanism in the MCCDC proposed earlier [7, 10] can be written,

$$CO_3^{2-} = CO_2 + 1/2\,O_2 + 2e \qquad (7)$$

Generally. the transport of carbon dioxide from the cathode to the anode in an electrochemical

concentrator can be described by the following series of processes:

(a) mass transfer of reactants through the cathode gas film,
(b) diffusion through cathode electrode,
(c) reaction at the interface,
(d) electrolyte transport through electrolyte,
(e) reaction at anode–electrolyte interface,
(f) diffusion through anode electrode, and
(g) mass transfer of products through anode gas film.

Under load, the anode pores fill with CO_2 and O_2 as they are produced. The nitrogen sweep gas offers little diffusional resistance in the bulk anode gas stream. Thus, activation should account for nearly all the anode overpotential;

$$i = i_o \left[\exp\left(\frac{\overleftarrow{\alpha} F}{RT} \eta\right) - \exp\left(-\frac{\vec{\alpha} F}{RT} \eta\right) \right] \quad (8)$$

At the cathode, on the other hand, diffusion of oxygen and CO_2 adds significantly to the overpotential [8]. A successful model for the cathodic process, based on a combination of bulk-phase mass-transfer, pore diffusion and electrochemical kinetics, was used by Weaver [8]. The revised Butler–Volmer expression is:

$$i = i_o \left[\exp\left(\frac{\overleftarrow{\alpha} F}{RT} \eta\right) - \left(1 - \frac{i}{i_L}\right) \exp\left(-\frac{\vec{\alpha} F}{RT} \eta\right) \right] \quad (9)$$

The limiting current density, i_L, is found to be determined by the diffusion of CO_2 from the oxidant gas to the active area [8]. This is due to the low concentration of CO_2 in the gas.

$$i_L = nFC^{\circ}/(1/k_g + \tau\delta/D\epsilon) \quad (10)$$

In the present work, Weaver's cathode equation was used unaltered, and Equation 8, with activation overpotential only, used for the anode. The characteristics of cell performance, i.e., the variation of cell potential with current, can be predicted from the mathematical model. Parameters i_o and i_L for the cathode and i_o for the anode are evaluated using non-linear regression.

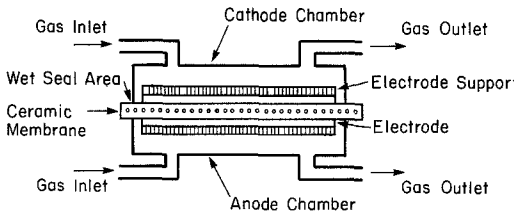

Fig. 1. Schematic diagram of the cell.

3. Experiments

Testing is needed both to verify the cathodic behaviour and to assess the anode performance with no fuel gas as depolarizer. That is, under conditions of a true concentration cell driven solely by electric power.

3.1. *Basic equipment*

A test of a high temperature MCCDC requires apparatus similar to that for a MCFC test, e.g. [6, 11–13]. Basic needs of both systems are: an electrochemical cell, a measurement system, and a furnace. The electrochemical cell itself consists of three main components: the cell housing, the electrodes and the electrolytic membrance or 'tile'. A typical cell is assembled as illustrated in Fig. 1.

The cell housing (Fig. 2) used was designed by the Institute of Gas Technology (IGT, [11]). The details and pretreatment are essentially the same. The superficial active electrode area is 7.9 cm^2.

Porous nickel electrodes of flat sheets of 80% porosity and 7.6 x 10^{-4} cm thickness with nickel screen for structural support were purchased from Gould, Inc. The membrane used in MCCDC tests is a mixture of alkali carbonate eutectic (62 mol% Li_2CO_3, 38 mol% K_2CO_3) 490° C, contained in a

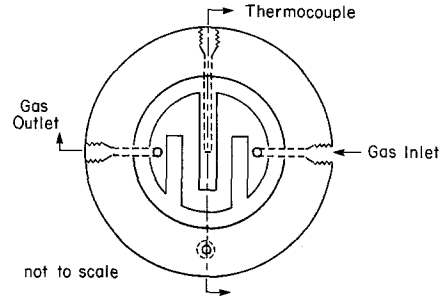

Fig. 2 Cell housing.

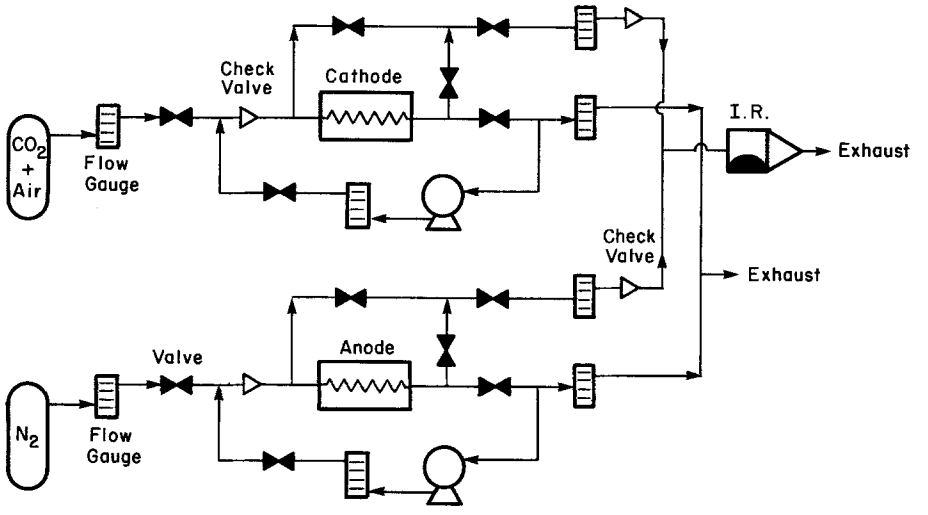

Fig. 3 Flow diagram for the process.

porous, non-conductive, and inert matrix of lithium aluminate ($LiAlO_2$) particles.

The reference electrode is a gold wire [8]. The wire is placed in alumina tubes for gas transport and a stainless steel tube for structural support. The coiled end of the gold wire is dipped in the lithium and potassium carbonate eutectic and bubbled with a reference gas containing 30% CO_2 in air.

The furnace and temperature control are essentially the same as that of Argonne National Laboratory (ANL, [14]).

3.2. *Measurement system*

A non-dispersive, flow infrared analyser was used for continuous monitoring of CO_2 from both anode and cathode chambers. A gas chromatograph was used intermittently to check these results.

Fig. 3 shows the flow diagram for this process. The system uses nitrogen as the product carrier on the anode side. A recycle pump is introduced in the cathode side to increase the velocity of process gas. Placing a recycle pump in the anode side could provide for increased concentration of CO_2 in the effluent gas. The flow meters on the inlet and outlet lines are used to check for leakage from the cell. All connections are made with steel or tygon tubing, Swagelok fittings, plastic tees, and tube-to-tube plastic connectors.

3.3. *Electronics*

The cell was operated with a precision galvanostat (PAE 371). Cell potentials, temperatures and CO_2 concentrations were continuously monitored on a multi-channel recorder. Ohmic polarizations were measured using current-interruption with aid of a storage oscilloscope.

3.4 *Operation*

Tests on the CO_2 concentrator have been conducted using a 1.25 inch (electrode diameter) cell from 500 to 600° C. A series of tests were conducted varying the cathodic flow rate from 125 to 2000 $cm^3\ min^{-1}$. The anodic flow rate was usually held constant at 80 $cm^3\ min^{-1}$ of nitrogen. Process gases supplied into the cathode were 0.25, 0.5 and 1% CO_2 in air. The reference gas for all tests was 30% CO_2 in air.

Heating was slowly accomplished while oxidant gases continually flowed over both electrodes. About 5 h were necessary to bring the cell to 600° C. The cell was left in this open-circuit condition for about two days before experiments were begun. This assured complete conversion of the electrodes to NiO. Lithiation occurred *in-situ*.

Current was applied in 10 mA increments. The voltage reading was taken when the apparent

steady-state was reached. A current-interruption technique was occasionally employed to estimate the IR-loss between reference and each electrode.

The current was increased step-wise until the cathode removal efficiency reached about 97%. A series of tests was conducted varying the cathodic flow rate from 125 to 2000 $cm^3\ min^{-1}$. The anodic flow rate was held constant at 80 $cm^3\ min^{-1}$ of nitrogen. The efficiencies (removal and current) and the cell overpotential were observed as a function of current densities, cathodic flow rates, and temperatures.

4. Results

The effects of process variables such as gas flow rates, CO_2 concentration, current density, and temperature on cell performance are reviewed. Current density is the current applied to the cell divided by the superficial area (7.92 cm^2) of the electrode.

4.1. *CO_2 removal from oxidant*

The basic performance criterion for the CO_2 concentrator, as used in a manned spacecraft, is the CO_2 removal efficiency. This is defined here as the percent of CO_2 at the cathode inlet which is removed in a single pass. Typical results are shown as Fig. 4. Removal efficiencies greater than 98% were routinely obtained.

At low currents, removal efficiency is nearly linear with current. As the current density is raised the flux of CO_2 is increased and the exiting cathode CO_2 partial pressure drops to very low levels.

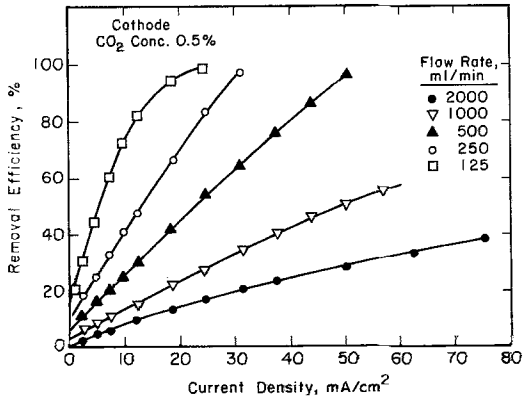

Fig. 4. CO_2 removal efficiency.

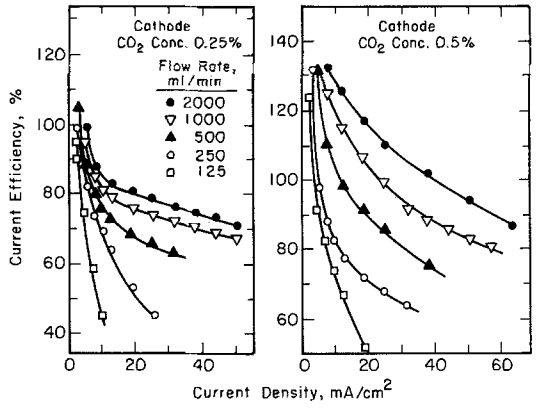

Fig. 5. Current efficiency versus current density.

This brings about a decrease in the rate of removal efficiency increase with current due to the decrease in mass-transfer driving force from the bulk gas stream.

Since there must be a flux of anions sufficient to carry the applied current, oxygen is reduced at a rate which is greater than the neutralization by CO_2. This produces a net flux of peroxide, superoxide and/or oxide to the anode. Here they are oxidized to oxygen. The net effect of operation at high current densities is a loss of current efficiency, here defined as the current required by Reaction (2) (two Faradays per mole of CO_2 transferred) divided by the actual current (× 100).

Current efficiency is plotted, for typical runs, in Fig. 5 for two inlet gas compositions. Values above 100% reflect other transfer mechanisms besides Reaction (2), as described earlier [7, 8]. They are chiefly due to diffusion from the cathode to anode caused by the positive concentration gradient in CO_2 at very low current. It is seen in

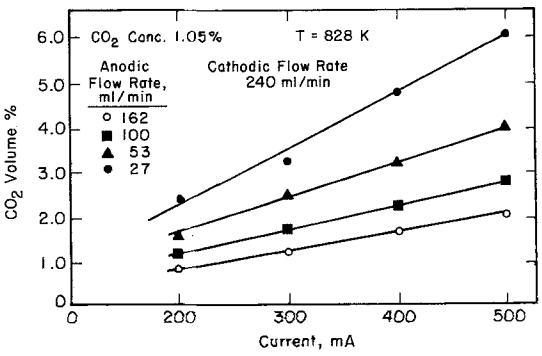

Fig. 6. CO_2 generation at anode for various anode flow rates as a function of current.

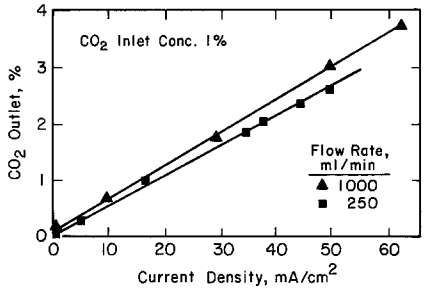

Fig. 7. Typical CO_2 generation from the anode for two cathode flow rates.

these graphs that, at high flows, the current efficiencies remain relatively high as current is increased. At low flows, however, the CO_2 is nearly completely removed from the oxidant. This, in turn, leads to significant oxy-anion transfer and lowered current efficiencies.

4.2. *Anode concentration*

Fig. 6 shows CO_2 generation from the anode for various anode flow rates as a function of current. Results in these plots indicate the CO_2 evolution from the anode is proportional to current load. An anodic flow rate of 27 cm^3 min^{-1} shows the highest CO_2 outlet concentration of 6.0 vol% at 500 mA.

Fig. 7 shows typical CO_2 generation from the anode for two cathode flow rates as a function of current density. A constant flow rate of 80 cm^3 min^{-1} was supplied to the anode. It is apparent that the CO_2 evolution at the anode is essentially independent of CO_2 inlet concentration at the cathode.

The relatively low concentrations of CO_2 produced are in no way indicative of process limitations. In this small, laboratory-scale device, insufficient CO_2 was transferred to permit high concentrations while still allowing for a reasonable flow of sweep nitrogen. A flow of 80 cm^3 min^{-1} was considered minimal to provide delivery to the infrared detector and gas chromatograph.

4.3. *Overpotentials*

Figs. 8–10 show experimental IR-free overpotentials at either electrode. The shapes of the curves are expected for an electrode with gas-phase mass-transfer control (cathode) and for one with gas evolution (anode). Complete mathematical treatment appears later.

The ohmic potential loss was regularly measured by current interruption. The apparent conductivity varied from 0.1 $(\Omega\,\mathrm{cm})^{-1}$ at 773 K to 0.02 $(\Omega\,\mathrm{cm})^{-1}$ at 873 K. This is quite low, suggesting ineffective contact between components.

5. Treatment of data

Equations 8 for the anode and 9 for the cathode describe the overal performance in terms of the gas-phase properties. The transfer coefficients ($\overleftarrow{\alpha}$ $\vec{\alpha}$) used were from the results of Winnick and Ross [10]. The parameters found are listed in Table 1.

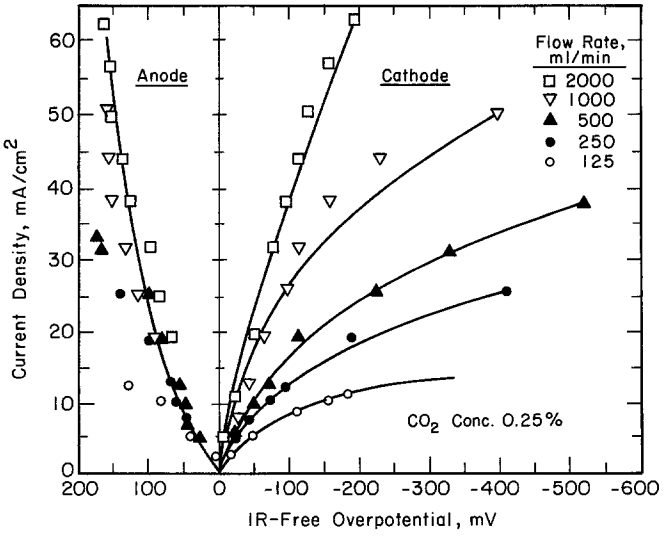

Fig. 8. Experimental IR-free overpotentials. Cell Performance: 0.25% CO_2 Feed. All curves calculated.

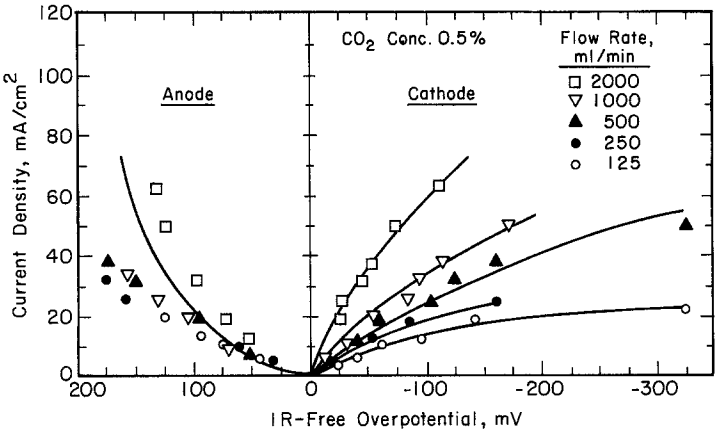

Fig. 9. Experimental IR-free overpotentials. Cell Performance: 0.50% CO_2 Feed. All curves calculated.

The experimental polarization data as well as the fit to Equations 8 and 9 are shown in Figs. 8–10.

5.1. *Cathode performance*

The cathode data exhibit exchange currents essentially the same as those found by Weaver [8]. There is no significant effect of CO_2 concentration, in keeping with the results of Ross [10]. The limiting currents increase with gas velocity and inlet CO_2 concentration, as expected. The diffusional resistance could not be accurately separated into the bulk-gas and pore contributions, Equation 10, due to the large change in $C^{\circ}(CO_2)$ from inlet to exit. However, the values for k_g and τ reported by Weaver [8] would adequately represent the data reported here.

The extent of activation polarization is shown for one case, 1% CO_2 at 1000 cm^3 min^{-1}. This curve is calculated with $i_L = \infty$.

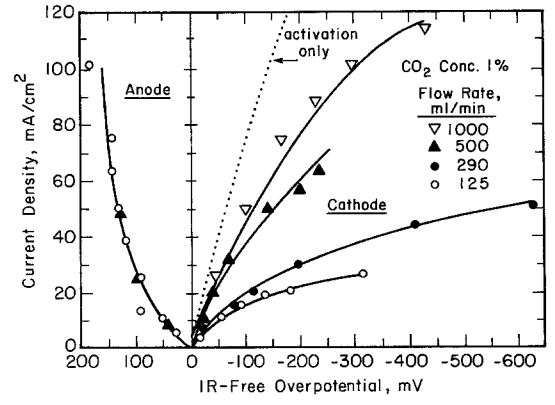

Fig. 10. Experimental IR-free overpotentials. Cell performance: 1.0% CO_2 Feed. All curves calculated.

5.2. *Anode performance*

The anode differes from the cathode in that gas is evolved during operation, rather than being absorbed from a finite source. Thus, the same reactant-limiting polarizations are not encountered. As explained above, the pores fill with 67% CO_2, 33% O_2 under load; the overpotential is essentially all due to activation. Of course, the equilibrium potential must be calculated on that basis. The electrode–electrolyte wetting, however, is different from that at the cathode. Thus, somewhat different values are found for i_o.

The anode polarizations as functions of current density are shown in Figs. 8–10. Since the exchange currents for the anode are practically constant, only one calculated curve is shown for the anode polarization. At the lower *cathode* inlet flow rates and large currents, it is seen that the anode polarization is higher than that calculated. This is probably due to transfer of oxide, as evidenced by the lowered CO_2 current efficiency, leading to a mixed oxidation reaction at the anode with,

$$O^{2-} \rightarrow 1/2\, O_2 + 2e \qquad (11)$$

in addition to Reaction (7).

6. Conclusions

Operation of the MCCDC driven cell appears to be suitable for the task of CO_2 removal from a manned spacecraft cabin. The driven cell performed at extremely low CO_2 partial pressures ($\geqslant$0.1 mmHg), showing high removal and current efficiencies.

Cathode CO_2 removal efficiencies of 97% were achieved with 0.25 CO_2 inlet concentration at

*Table 1. Fitted parameters***‡*

Inlet CO_2 (%)	*Flow Rate ($cm^3\ min^{-1}$)*	*Cathode i_o ($mA\ cm^{-2}$)*	*i_L ($mA\ cm^{-2}$)*	*Anode§ i_o ($mA\ cm^{-2}$)*
0.25	125	16.0	13.2	4.0
0.25	250	13.1	29.4	4.2
0.25	500	15.0	41.4	5.2
0.25	1000	27.5	57.1	4.0
0.25	2000	24.9	220.0	4.9
0.50	125	15.9	27.8	3.1
0.50	250	21.2	34.9	3.6
0.50	500	20.0	81.2	6.8
0.50	1000	23.1	180.0	4.0
0.50	2000	41.0	350.0	5.0
1.0	125	16.3	34.2	*
1.0	290	15.2	54.9	*
1.0	500	29.0	138.0	*
1.0	1000	38.7	141.0	4.3

*Unusually high polarizations precluded realistic estimate.
**All runs at 873 K.
† All inlet gases contained 21% oxygen, remainder nitrogen
‡ $\overleftarrow{\alpha} = 1.5$, $\overrightarrow{\alpha} = 0.5$ for all runs.
§ Equilibrium potential calculated based on 67% CO_2, 33% O_2 in anode under load.

19 mA cm^2 at operating temperatures near 873 K. For 0.5% CO_2, a removal efficiency of 90% was achieved at the same operating conditions.

Anode CO_2 concentrations of up to 5.8% were obtained. Higher anode CO_2 concentrations were not seen due to anode sweep-gas flow limitations.

Current efficiencies ranged from above 100% to below 50%, based on CO_2 transport. Those above 100% were due to non-electrochemical CO_2 utilization, mostly diffusion. Those below 100% were due to oxy-anion transport at higher current densities. This, in turn, is caused by CO_2 mass transfer limitations in the low-concentration oxidant-gas phase.

Simple cathode and anode performance equations have been applied to correlate cell performance. They agree well with those measured experimentally, reproducing the effects of current density, flow rate and CO_2 inlet concentration. Electrode polarization predictions using the models were separated into activation and diffusion polarizations. Diffusion polarization is generally lower than activation polarization, as expected.

Anodic performance showed lower exchange current densities and higher polarization than the cathode. These results suggest poor electrode wetting and a small active area. Calculated total polarizations show excellent agreement with experimental polarizations.

Acknowledgement

The authors wish to thank Mr P. D. Quattrone (now deceased) for his assistance. The work was funded, in part, by the NASA Ames Research Center, to whom we are grateful. The electrolyte tiles (membranes) were donated by the General Electric Company.

References

[1] J. L. Weaver, 'Electrochemical Molten Carbonate Carbon Dioxide Concentrator' MS thesis, Georgia Institute of Technology, Atlanta, GA (1981).
[2] L. Dellosso, J. Ruder and J. Winnick, *I/EC Proc. Des. Dev.* 8 (1969) 477.
[3] J. E. Clifford, *et al.*, 'A Water Vapor Electrolysis Cell with Phosphoric Acid Electrolyte,' NASA CR-73170, Battelle Memorial Institute, September (1966).
[4] J. Winnick, R. D. Marshall and F. H. Schubert, 'An Electrochemical Device for Carbon Dioxide Concentration. I. System Design and Performance' *Ind. Eng. Chem. Proc. Des. Dev.* **31** (1974) 59.
[5] G. H. J. Broers, 'High Temperature Galvanic Fuel Cells' PhD Thesis, University of Amsterdam, Netherlands (1958).
[6] Institute of Gas Technology, Project 9105, Final

Report, April, 1979.
[7] J. Winnick, H. Toghiani and P. Quattrone, *AIChE* **28** (1982) 103.
[8] J. L. Weaver and J. Winnick, *J. Electrochem. Soc.* **130** (1983) 20.
[9] A. J. Appleby and S. Nicholson, *J. Electronanal. Chem. Interfacial Electrochem.* **53** (1974) 105.
[10] J. Winnick and P. N. Ross, Jr, *J. Electrochem. Soc.* **128** (1981) 991.
[11] Institute of Gas Technology, 'Development of Molten Carbonate Fuel Cells' AGA Project DC-4-1, Final Report, Chicago (1967).
[12] Institute of Gas Technology, Project 8984, Quarterly Report, July–September, 1976; Quarterly Report, October–December, 1976.
[13] United Technologies Corporation, EPRI EM-856, Project 114-2, December 1978.
[14] J. P. Ackerman, K. Kinoshita, J. W. Sim, R. Swaroop, and P. A. Nelson, 'Advanced Fuel Cell Development' Contract W-31-109-Eng-38, Argonne National Laboratories, Progress Reports No. ANL-77-29, March 1977; No. ANL-77-56, June 1977; and ANL-78-71, August 1978.